

Determination of the Packing Mode of the Coiled-Coil Domain of cGMP-Dependent Protein Kinase α in Solution Using Charge-Predicted Dipolar Couplings

Markus Zweckstetter, Jason R. Schnell, and James J. Chou*

Max Planck Institute for Biophysical Chemistry, Am Fassberg 11, 37077 Göttingen, Germany, and Department of Biological Chemistry and Molecular Pharmacology, Harvard Medical School, Boston, Massachusetts 02115

Received May 27, 2005; E-mail: james_chou@hms.harvard.edu

Coiled-coil motifs are ubiquitous in biology and play essential roles in protein assembly and molecular recognition and are, therefore, the targets of many ongoing structural and functional studies.¹ The highly conserved structural features of coiled-coils are often exploited in predicting the atomic coordinates of this class of protein from the primary sequence. However, it is not possible to derive, using a knowledge-based approach, a unique solution for the relative orientation of subunit packing. Although the majority of coiled-coil dimers are parallel, there are a growing number of antiparallel cases in the database. Current methods for establishing the packing mode of coiled-coil proteins are labor-intensive and involve introducing disulfide bonds² or synthetic spin-labels.³

In an earlier study, we explored the utility of combining knowledge-based coiled-coil packing distances and orientation constraints derived from NMR residual dipolar couplings (RDCs) for rapid determination of the solution structure of a coiled-coil dimer without carrying out the time-consuming procedure of analyzing Nuclear Overhauser Enhancement (NOE) spectra.⁴ It was found that both parallel and antiparallel models could be constructed from the information given in the Protein Data Bank (PDB), and that both agreed equally well with experimental RDCs. Here, we show that the relative subunit orientation of coiled-coil proteins in solution can be determined without chemical modification by comparison of RDCs measured in charged liquid-crystalline medium with values predicted from the three-dimensional charge distribution of the protein. The method is demonstrated for the coiled-coil domain of the cGMP-dependent protein kinase α (cGK1 α), a protein responsible for mediating the interaction between the kinase and the myosin-binding subunit of myosin phosphatase.⁵

Sizable one-bond internuclear dipolar couplings can be measured for proteins weakly aligned in liquid-crystalline medium.⁶ Recently, it has been reported that when using charged liquid-crystalline medium formed by filamentous phage (Pf1) particles to partially align biological macromolecules, the magnitude and orientation of the protein's alignment tensor can be predicted with reasonable accuracy from the three-dimensional charge distribution and shape of the macromolecule.^{7,8} A highly simplified model was developed, which approximates the electrostatic interaction between a solute and an ordered phage particle as that between the solute surface charges and the electric field of the phage. The solute, represented by effective charges q_i placed at the positions r_i of its ionizable residues, was treated as a particle in the external field of the liquid crystal, and its electrostatic potential $\varphi(\mathbf{r})$ was obtained by solving the nonlinear three-dimensional Poisson–Boltzmann equation. The distance and orientation-dependent electrostatic free energy was approximated by $\Delta G_{\text{el}}(\mathbf{r}, \mathbf{\Omega}) = \sum_i q_i \varphi[\mathbf{r}_i(\mathbf{r}, \mathbf{\Omega})]$. The Boltzmann factor $p_B(\mathbf{r}, \mathbf{\Omega}) = \exp[-\Delta G_{\text{el}}(\mathbf{r}, \mathbf{\Omega})/k_B T]$ provided relative electrostatic weights when averaging individual alignment tensors, derived for each orientation and distance:

$$A_{ij} = 1/2 (3 \cos \theta_i \cos \theta_j - \delta_{ij}) \quad (i, j = x, y, z) \quad (1)$$

yielding an overall solute alignment tensor

$$A_{ij}^{\text{struc}} = \int A_{ij} p_B(\mathbf{r}, \mathbf{\Omega}) \, d\mathbf{r} \, d\mathbf{\Omega} / \int p_B(\mathbf{r}, \mathbf{\Omega}) \, d\mathbf{r} \, d\mathbf{\Omega} \quad (2)$$

In eq 1, θ_i denotes the angle between the i th molecular axis and the direction of magnetic field and δ_{ij} the Kronecker delta. In the present study, we extended this approach by averaging A_{ij}^{struc} over an ensemble of K protein conformers, obtained from NMR structure refinement, to account for structural uncertainty and dynamics, yielding a final protein alignment tensor

$$A_{ij}^{\text{mol}} = \sum_K A_{ij}^{\text{struc}} \quad (3)$$

The predicted one-bond RDC between a pair of spin 1/2 nuclei, P and Q, in the protein (${}^1D_{PQ}$) can then be computed from A_{ij}^{mol} .

To determine the monomer–monomer orientation of the coiled-coil domain of cGK1 α , the high-resolution structure of the rigid segment encompassing the coiled-coil (residues 9–44) was determined by RDC-based molecular fragment replacement.^{4,9} A close structural model was first selected by fitting ${}^1D_{\text{NH}}$, ${}^1D_{\text{C}\alpha}$, and ${}^1D_{\text{CN}}$ of cGK1 α^{9-44} , measured in Pf1 medium, to all 36-residue segments of the 2.7 Å crystal structure of the 14-heptad-repeat coiled-coil domain of cortexillin I from *Dictyostelium discoideum*.¹⁰ To define the subtle helix curvature specific to cGK1 α^{9-44} , the selected crystal structure was further refined against experimental RDCs using a low-temperature simulated annealing protocol as described by Schnell et al.⁴ Since RDCs were measured for protein containing residues 1–59 of cGK1 α and 8 residues at the N-terminus from cloning (see Figure 1), of which the non-native segment and residues 1–4 and 49–59 of cGK1 α are dynamic as previously indicated by ${}^{15}\text{N}$ relaxation rates,⁴ the entire polypeptide chain (67 residues long) was used during structure calculation. However, experimental restraints were applied only to the more or less rigid segment (residues 5–48 of cGK1 α). Antiparallel and parallel dimeric coiled-coil models were then built with knowledge-based intermonomer distance restraints.

Due to the inherent 4-fold orientational degeneracy of RDCs and the molecular symmetry of the coiled-coil structure, RDC refinement alone cannot be used to distinguish between parallel and antiparallel packing of cGK1 α^{5-48} . The overall shapes of the parallel and antiparallel structures are very similar (Figure 1). Hence, methods that attempt to distinguish the two packing modes based on the overall dimension of the structures are likely to fail. Indeed, when using a purely steric obstruction model to predict solute alignment on the basis of molecular shape,⁷ the two models (residues 5–48 of cGK1 α) yield almost identical RDCs. The alignment tensors are both axially symmetric, with a magnitude of

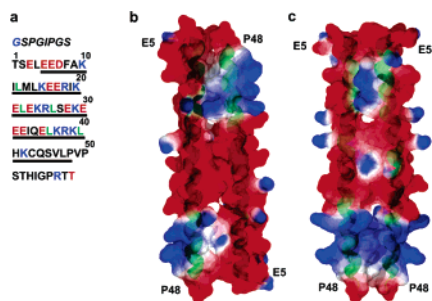


Figure 1. The coiled-coil region of cGK1 α . (a) Sequence with acidic and basic residues colored in red and blue, respectively. Leucines and isoleucines in heptad positions *a* and *d* are shown in green. This sequence includes 8 residues at the N-terminus from the cloning. The bar denotes the well-structured coiled-coil region; (b) and (c) are electrostatic surface models of the antiparallel and parallel homodimer, respectively.

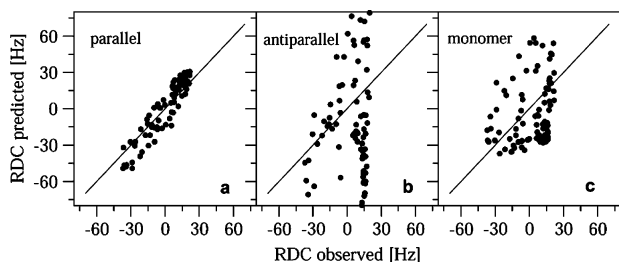


Figure 2. Correlations between experimental $^1D_{\text{NH}}$, $^1D_{\text{CC}\alpha}$, and $^1D_{\text{CN}}$ values and values predicted from the three-dimensional charge distributions and shapes of different stoichiometries and relative arrangements of cGK1 α . (a) The parallel homodimer, (b) the antiparallel homodimer, and (c) the monomer.

-11.4 ± 0.2 and -11.3 ± 0.2 Hz for the parallel and antiparallel structure, respectively.

Although, parallel and antiparallel dimers have similar shapes and identical net charges, very different charge distributions are associated with the two structural models (Figure 1). The acidic and basic residues are primarily located in the N- and C-terminal half of cGK1 α , respectively, such that the parallel dimer possesses a large dipole moment of 489 ± 28 D. For the antiparallel arrangement, on the other hand, positive and negative charges are proximal, and the dipole moment amounts to only 86 ± 31 D. In addition, the orientation of the multipole moments of the parallel and antiparallel arrangements differ by about 80° for the dipole vector and about 30° for the generalized¹¹ quadrupole vector.

Figure 2 compares the measured RDCs with values predicted from the charge distribution and shape of the parallel dimer, the antiparallel dimer, and the monomer structure of cGK1 α ^{5–48}. RDCs predicted from the parallel dimer fit very well to experimental values with a linear correlation coefficient *r* of 0.94 (Figure 2a). A very different alignment tensor, on the other hand, is predicted for the antiparallel dimer, and charge-shape-predicted RDCs differ strongly from experimental values (*r* = 0.39) (Figure 2b). Finally, experimental RDCs do not correlate with values predicted from the monomer structure (*r* = 0.21) (Figure 2c). The above indicate that the coiled-coil region of cGK1 α forms a parallel homodimer in solution.

The excellent agreement between predicted and observed RDCs for the parallel dimer of cGK1 α suggests that charges located in the flexible termini (N terminus, E3, R57, and C terminus), which were not included in the calculations, do not significantly contribute to the observed alignment. RDCs may also be predicted when

including all 23 flexible residues. Since the flexible tails sample a large conformational space that could lead to large variations in predicted alignment tensors, a total of 300 different conformations were calculated for both the parallel and antiparallel dimer, but only the 30 structures that individually gave the best fit between charge-shape-predicted and experimental RDCs were averaged (eq 3). Again, only RDCs predicted for the parallel dimer fit reasonably well to experimental values (*r* = 0.74 for the parallel and *r* = 0.23 for the antiparallel dimer), suggesting that the distinction between the two arrangements is robust. If 60 best-fitting structures were considered, *r* = 0.59 and 0.23 for the parallel and antiparallel dimer, respectively.

To obtain high-resolution structural details of the constituent helices of cGK1 α , three types of backbone RDCs and side chain χ_1 angles were used for the structure calculations.⁴ However, when the major aim is the determination of the global arrangement of the constituent helices and not their detailed local structure, only a small set of $^1D_{\text{NH}}$ couplings is sufficient. The same approach was used, but with only 33 $^1D_{\text{NH}}$ couplings, to refine and assemble cGK1 α monomers into parallel and antiparallel homodimers, which could then be distinguished (RDC correlations of 0.74 and -0.20 for the parallel and antiparallel dimer, respectively).

This report demonstrates that the relative arrangement of constituent monomers within coiled-coil dimers can be determined rapidly in solution by comparison of experimental RDCs with values predicted from the 3D charge distribution of different multimeric models of the protein. Since, as is the case for cGK1 α , charged residues are frequently found at the “e” and “g” positions of coiled-coil heptad repeats, this method of discriminating between packing modes is expected to be general. For coiled-coil proteins, a full-scale structure determination of the monomer is not required a priori, as it can be easily obtained from the known coiled-coil structures by the RDC-based molecular replacement method. We anticipate that the method introduced here can be extended to determine the relative orientation and stoichiometry of other types of multimeric protein assembly.

Acknowledgment. M.Z. is supported by a DFG Emmy Noether Grant (ZW 71/1-4). J.J.C. is supported by Smith Family Award for Young Investigators and the PEW Scholarship.

Supporting Information Available: Materials and methods section and additional tables. This material is available free of charge via the Internet at <http://pubs.acs.org>.

References

- (1) (a) Newman, J. R.; Wolf, E.; Kim, P. S. *Proc. Natl. Acad. Sci. U.S.A.* **2000**, *97* (24), 13203. (b) Lupas, A.; Van Dyke, M.; Stock, J. *Science* **1991**, *24* (252), 1162.
- (2) (a) Hodges, R. S.; Saund, A. K.; Chong, P. C.; St-Pierre, S. A.; Reid, R. E. *J. Biol. Chem.* **1981**, *256* (3), 1214. (b) O’Shea, E. K.; Rutkowski, R.; Kim, P. S. *Science* **1989**, *243* (4890), 538.
- (3) Hillar, A.; Tripet, B.; Zoetewey, D.; Wood, J. M.; Hodges, R. S.; Boggs, J. M. *Biochemistry* **2003**, *42* (51), 15170.
- (4) Schnell, J. R.; Zhou, G.; Zweckstetter, M.; Rigby, A. C.; Chou, J. J. *Protein Sci.* **2005**, in press.
- (5) Surks, H. K.; Mendelsohn, M. E. *Cell. Signalling* **2003**, *15*, 937.
- (6) Tjandra, N.; Bax, A. *Science* **1997**, *278* (5340), 1111.
- (7) Zweckstetter, M.; Bax, A. *J. Am. Chem. Soc.* **2000**, *122*, 3791.
- (8) Zweckstetter, M.; Hummer, G.; Bax, A. *Biophys. J.* **2004**, *86*, 3444.
- (9) Delaglio, F.; Kontaxis, G.; Bax, A. *J. Am. Chem. Soc.* **2000**, *122* (9), 2142.
- (10) Burkhard, P.; Kammerer, R. A.; Steinmetz, M. O.; Bourenkov, G. P.; Aebi, U. *Structure* **2000**, *8*, 223.
- (11) Sass, J.; Cordier, F.; Hoffmann, A.; Rogowski, M.; Cousin, A.; Omichinski, J. G.; Lowen, H.; Grzesiek, S. *J. Am. Chem. Soc.* **1999**, *121* (10), 2047.

JA0534654